Acta Cryst E CRYSTALLOGRAPHIC COMMUNICATIONS

ISSN 2056-9890

Crystal structure and Hirshfeld surface analysis of (2^2*RS*,2^3*SR*,2^5*RS*,2^6*SR*)-2^3,2^5,5-trimethyl-2^1-(2,2,2-trifluoroacetyl)-5-aza-2(2,6)-piperidina-1,3(2,5)-difuranacyclohexaphan-2^4-one

Sema Öztürk Yıldırım,[a,b] Mehmet Akkurt,[b] Anastasia A. Ershova,[c] Mikhail S. Grigoriev,[d] Bruno G.M. Rocha[e] and Ajaya Bhattarai[f]*

[a]Department of Physics, Faculty of Science, Eskisehir Technical University, Yunus Emre Campus 26470 Eskisehir, Türkiye, [b]Department of Physics, Faculty of Sciences, Erciyes University, 38039 Kayseri, Türkiye, [c]Peoples' Friendship University of Russia (RUDN University), 6 Miklukho-Maklaya St., Moscow, 117198, Russian Federation, [d]Frumkin Institute of Physical Chemistry and Electrochemistry, Russian Academy of Sciences (IPCE RAS), 31 Bldg 4, Leninsky prosp., Moscow, 119071, Russian Federation, [e]Centro de Química Estrutural, Institute of Molecular Sciences, Instituto Superior Técnico, Universidade de Lisboa, Av. Rovisco Pais, 1049-001 Lisboa, Portugal, and [f]Department of Chemistry, M.M.A.M.C (Tribhuvan University), Biratnagar, Nepal. *Correspondence e-mail: ajaya.bhattarai@mmamc.tu.edu.np

Received 1 February 2023
Accepted 2 March 2023

Edited by B. Therrien, University of Neuchâtel, Switzerland

Keywords: crystal structure; twelve-membered heterocycles; furan; alkylation; piperidon; Hirshfeld surface analysis; Mannich reaction.

CCDC reference: 2245808

Supporting information: this article has supporting information at journals.iucr.org/e

The title compound, $C_{20}H_{21}F_3N_2O_4$, features a main twelve-membered difuryl ring with which the furan rings make dihedral angles of 76.14 (5) and 33.81 (5)°. The dihedral angle between the furan rings is 42.55 (7)°. The six-membered nitrogen heterocycle has a twist-boat conformation. In the crystal, pairs of molecules are connected by intermolecular C—H···O interactions, generating an $R_2^2(14)$ ring motif. These pairs of molecules form *zigzag* chains along the *a*-axis direction by means of C—H···F interactions. Furthermore, C—H···π and C–F···π interactions link the molecules into chains along the *b*-axis direction, forming sheets parallel to the (001) plane. These sheets are also connected by van der Waals interactions.

1. Chemical context

Twelve-membered aza- and oxa-macrocycles possess a wide range of useful biological activities and exhibit a tendency to bind metal cations with their macrocyclic cavities (Simonov *et al.*, 1993). For example, well-known naturally occurring macrocycles such as enniatins demonstrate a high cytotoxic activity (Levy *et al.*, 1995; Ivanova *et al.*, 2006) and aza-tri(tetra)pyrrolic macrocycles can be used as ion-pair receptors (Yadigarov *et al.*, 2009). Chiral macrocycles with multiple non-covalent bonding sites show chiral recognition to different anions (Ema *et al.*, 2014; Khalilov *et al.*, 2021; Maharramov *et al.*, 2010). S,N-Containing macrobicyclic aza-cryptands (Khabibullina *et al.*, 2018; Naghiyev *et al.*, 2020; Safavora *et al.*, 2019) including dipyrrolylmethane subunits in their structures exhibit a high affinity to anions, especially the fluoride ion (Guchhait, *et al.*, 2011; Shikhaliyev *et al.*, 2018, 2019) and can be used as chemical delivery systems.

On the other hand, the Mannich reaction is an extensively used method for the construction of various types of polycyclic systems (Rivera *et al.*, 2015; Ma *et al.*, 2021; Mahmoudi *et al.*, 2016), including those containing pyrroles (Jana *et al.*, 2019). In order to create a short pathway to macrocycles possessing two different donating atoms in a twelve-membered ring, we used an acid-catalysed Mannich type reaction between 2,6-difuryl-substituted piperidone and *N*-substituted 1,5,3-diox-

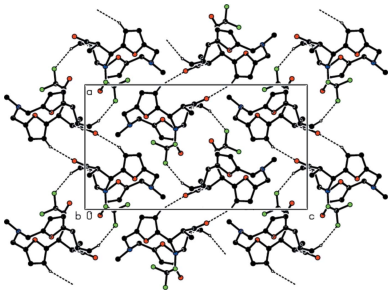

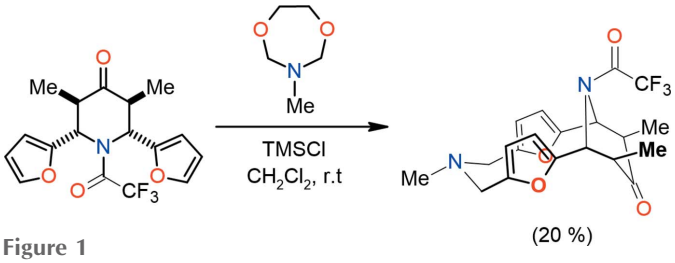

Figure 1
The synthetic route.

azepane (Fig. 1). The main goal of this study was to obtain the first representative of a twelve-membered difuryl containing rings and to establish its stereochemistry and non-covalent bond donor or acceptor ability (Gurbanov *et al.*, 2020*a*,*b*; Mahmudov *et al.*, 2021, 2022). The rings formed in this transformation can serve as precursors for studying the IMDAV (intramolecular Diels–Alder reaction of vinylarenes; Krishna, *et al.*, 2022) and IMDAF (intramolecular Diels–Alder reaction of furans; Kvyatkovskaya *et al.*, 2021*a*,*b*; Borisova, *et al.*, 2018) reactions.

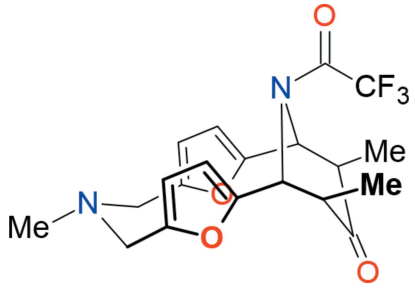

2. Structural commentary

As shown in Fig. 2, the title compound has a main twelve-membered difuryl-containing ring (O18 /C2/C1/N17/C13/C12/O19/C9/C8/N7/C6/C5) to which the furan rings (O18/C2–C5 and O19/C9–C12) subtend dihedral angles of 76.14 (5) and 33.81 (5)°, respectively. The dihedral angle subtended by the furan ring is 42.55 (7)°. The six-membered nitrogen heterocycle (N17/C1/C13–C16) adopts a twist-boat conformation with puckering parameters (Cremer & Pople, 1975) Q_T = 0.6999 (12) Å, θ = 90.12 (10)° and φ = 228.08 (10)°.

Table 1
Hydrogen-bond geometry (Å, °).

*Cg*2 is the centroid of the O19/C9–C12 ring.

D—H···*A*	*D*—H	H···*A*	*D*···*A*	*D*—H···*A*
C3—H3···O15^{i}	0.95	2.51	3.3809 (15)	152
C20—H20*B*···F3^{ii}	0.98	2.54	3.4700 (16)	160
C21—H21*B*···*Cg*2^{iii}	0.98	2.88	3.7561 (13)	150

Symmetry codes: (i) $-x, -y+1, -z+1$; (ii) $-x+1, -y+1, -z+1$; (iii) $-x+\frac{1}{2}, y-\frac{1}{2}, z$.

3. Supramolecular features and Hirshfeld surface analysis

In the crystal, pairs of molecules are connected by intermolecular C—H···O interactions, forming an $R_2^2(14)$ ring motif (Bernstein *et al.*, 1995). These pairs of molecules form zigzag chains along the *a*-axis direction by C—H···F interactions (Table 1, Fig. 3). Furthermore, C—H···π and C—F···π interactions [C18—F1···*Cg*1^{i}, C18···*Cg*1^{i} = 3.9574 (14) Å, F1···*Cg*1^{i} = 3.5265 (9) Å, C18—F1···*Cg*1^{i} = 98.83 (6)° and C18—F3···*Cg*1^{i}, C18···*Cg*1^{i} = 3.9574 (14) Å, F1···*Cg*1^{i} = 3.5496 (11) Å, C18—F1···*Cg*1^{i} = 97.90 (7)° where *Cg*1 is the centroid of the O18/C2–C5 ring; symmetry code: (i) $\frac{1}{2}+x, y, \frac{3}{2}-z$] link the molecules into chains along the *b*-axis direction, forming sheets parallel to the (001) plane (Table 1, Fig. 4). These sheets are also connected by van der Waals interactions.

Crystal Explorer17.5 (Turner *et al.*, 2017) was used to perform a Hirshfeld surface analysis and to create the corresponding two-dimensional fingerprint plots, with the three-dimensional d_{norm} surfaces plotted at a standard reso-

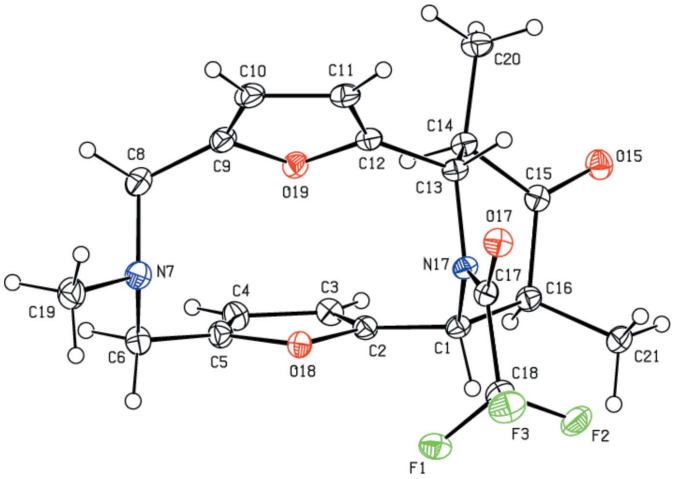

Figure 2
Molecular structure of the title compound. Displacement ellipsoids are drawn at the 30% probability level.

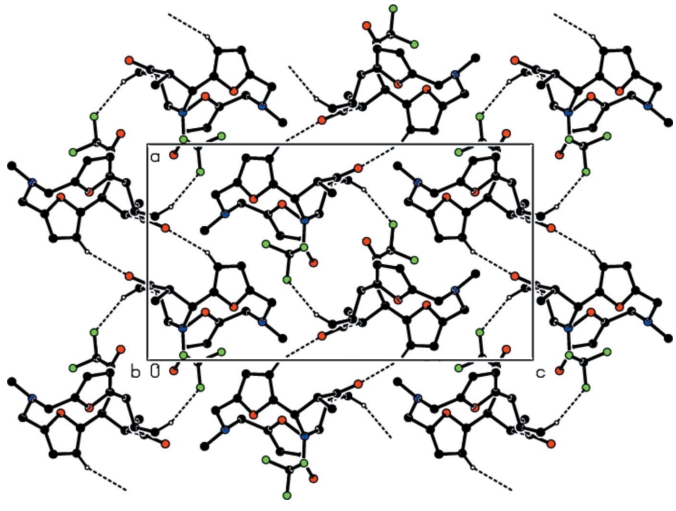

Figure 3
View down the *b*-axis showing the C—H···O and C—H···F hydrogen bonds (dashed lines).

Table 2
Summary of short interatomic contacts (Å) in the title compound.

N7···H4	2.71	$\frac{1}{2}+x, y, \frac{3}{2}-z$
F2···H19*C*	2.65	$1-x, -\frac{1}{2}+y, \frac{3}{2}-z$
H20*B*···F3	2.54	$1-x, 1-y, 1-z$
H21*A*···H19*A*	2.46	$\frac{1}{2}-x, 1-y, -\frac{1}{2}+z$
H20*A*···H16	2.48	$-x, 1-y, 1-z$
H20*C*···H21*B*	2.50	$\frac{1}{2}-x, \frac{1}{2}+y, z$
H20*A*···H11	2.53	$-\frac{1}{2}+x, \frac{3}{2}-y, 1-z$

lution of −0.1525 (red) to 1.7277 (blue) a.u (Fig. 5). The bright-red patches near atoms O15 and H20*B* on the Hirshfeld surface represent weak C—H···O and C—H···F interactions (Tables 1 and 2).

The fingerprint plots (Fig. 6) show that H···H (44.9%), F···H/H···F (23.0%), O···H/H···O (16.7%) and C···H/H···C (8.5%) interactions contribute the most to surface contacts. The crystal packing is additionally influenced by F···C/C···F (3.0%), N···H/H···N (1.4%), F···O/O···F (0.9%), C···O/O···C (0.9%), O···O (0.5%) and C···C (0.1%) interactions. The Hirshfeld surface study confirms the significance of H-atom interactions in the packing formation. The large number of H···H, F···H/H···F, O···H/H···O and C···H/H···C interactions indicate that van der Waals interactions and hydrogen bonding are important in the crystal packing (Hathwar *et al.*, 2015).

4. Database survey

1,8,12,19,24,26-Hexaazapentacyclo[17.3.1.13,6.18,12.114,17]-hexacosa-3,5,14,16-tetraene ethyl acetate solvate dihydrate (CSD refcode NOYCOW; Jana *et al.*, 2019) is the most similar compound to the title found in a search of the Cambridge Structural Database (CSD, Version 5.42, update of September 2021; Groom *et al.*, 2016). It crystallizes in the monoclinic space group *I*2/*a* (15) with $Z = 8$. The two pyrrolic NH atoms are oriented in the same direction. It exhibits a different

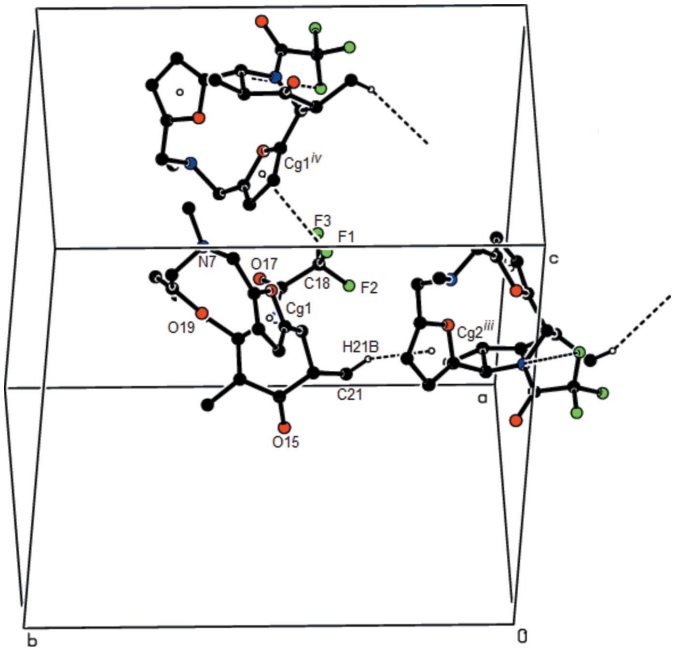

Figure 4
A general view in the unit cell of the C—H···π and C—F···π interactions (dashed lines). Symmetry codes: (iii) $-x+\frac{1}{2}, y-\frac{1}{2}, z$; (iv) $\frac{1}{2}+x, y, \frac{3}{2}-z$.

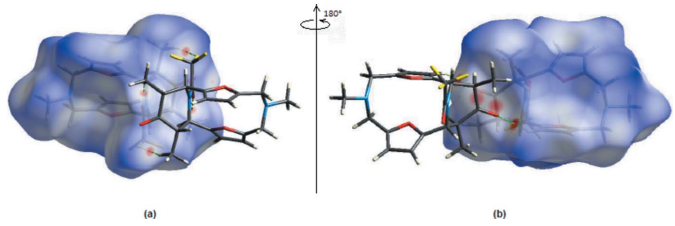

Figure 5
(*a*) Front and (*b*) back views of the three-dimensional Hirshfeld surfaces of the title molecule.

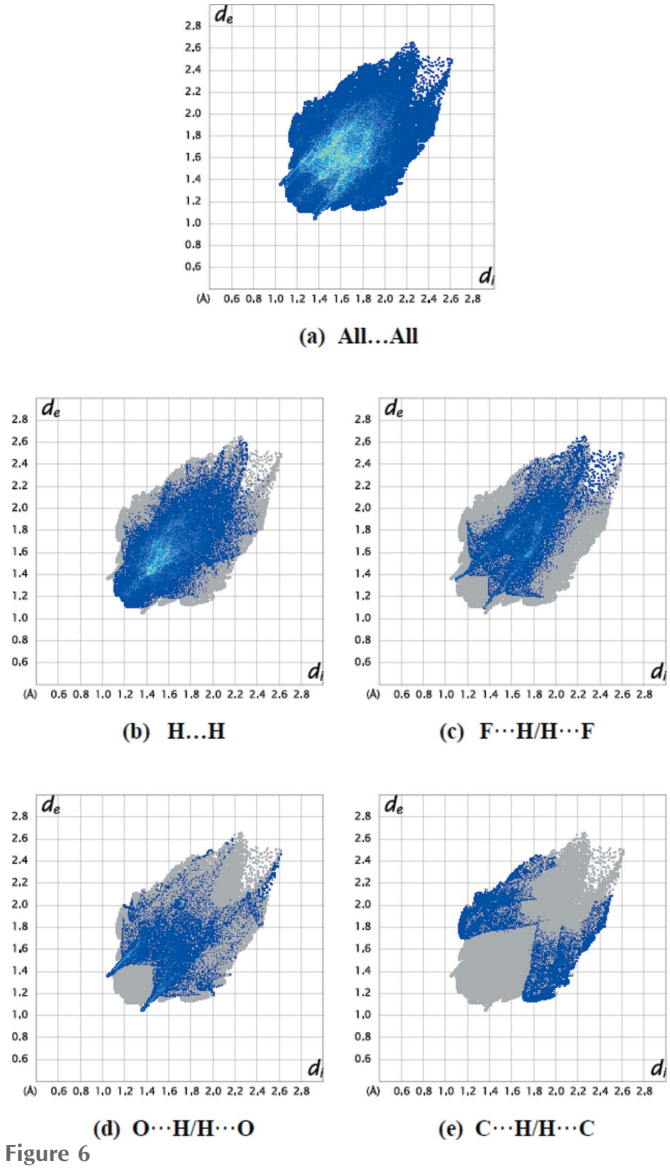

Figure 6
Two-dimensional fingerprint plots for title molecules showing (*a*) all interactions, and delineated into (*b*) H···H, (*c*) F···H/H···F, (*d*) O···H/H···O and (*e*) C···H/H···C interactions. The d_i and d_e values are the closest internal and external distances (in Å) from given points on the Hirshfeld surface.

Table 3
Experimental details.

Crystal data	
Chemical formula	$C_{20}H_{21}F_3N_2O_4$
M_r	410.39
Crystal system, space group	Orthorhombic, *Pbca*
Temperature (K)	100
a, *b*, *c* (Å)	11.1351 (1), 17.0545 (2), 19.9131 (3)
V (Å^3)	3781.57 (8)
Z	8
Radiation type	Cu *Kα*
μ (mm^{-1})	1.03
Crystal size (mm)	0.25 × 0.20 × 0.20
Data collection	
Diffractometer	XtaLAB Synergy, Dualflex, HyPix
Absorption correction	Multi-scan (*CrysAlis PRO*; Rigaku OD, 2021)
T_{min}, T_{max}	0.761, 0.801
No. of measured, independent and observed [$I > 2\sigma(I)$] reflections	24690, 4040, 3752
R_{int}	0.031
(sin $\theta/\lambda)_{max}$ (Å^{-1})	0.637
Refinement	
$R[F^2 > 2\sigma(F^2)]$, $wR(F^2)$, *S*	0.037, 0.102, 1.03
No. of reflections	4040
No. of parameters	265
H-atom treatment	H-atom parameters constrained
$\Delta\rho_{max}$, $\Delta\rho_{min}$ (e Å^{-3})	0.32, −0.21

Computer programs: *CrysAlis PRO* (Rigaku OD, 2021), *SHELXT* (Sheldrick, 2015*a*), *SHELXL2018* (Sheldrick, 2015*b*), *ORTEP-3 for Windows* (Farrugia, 2012) and *PLATON* (Spek, 2020).

conformation from the title compound: the furan rings in the title compound are almost normal to the mean plane of the main twelve-membered difuryl-containing ring and their oxygen atoms are oriented to the opposite sides whereas in NOYCOW, they are also almost normal, but are on the same side.

5. Synthesis and crystallization

A mixture of *N*-trifluoro-acylated piperodone (2.6 mmol), 3-methyl-1,5,3-dioxazepane (2.7 mmol) and Me_3SiCl (1.1 mL, 8.6 mmol) in dry dichloromethane (CH_2Cl_2) (5 mL) was left for 5 days under an argon atmosphere without stirring. The reaction mixture was then poured into water (30 mL) and basified with solid K_2CO_3 until the pH was 9–10. The organic products were extracted with CH_2Cl_2 (2 × 20 mL) and dried over anhydrous Na_2SO_4. After evaporation of the solvent, the crude residue was purified by column chromatography on silica gel (ethyl acetate/hexane, from 1:20 to 1:4) and then the resulting solid fractions were recrystallized from a chloroform/hexane mixture to give the macrocycle as a white solid. Single crystals were obtained by slow crystallization from a hexane/chloroform mixture.

Yield 20% (0.21 g), m.p. 420–422 K. ^{1}H NMR (700 MHz, $CDCl_3$) δ (*J*, Hz): 6.24 (*br.s*, 2H), 6.19 (*br.s*, 1H), 6.02 (*d*, *J* = 2.9 Hz, 1H), 5.28 (*s*, 1H), 5.11 (*d*, *J* = 9.5 Hz, 1H), 3.86 (*d*, *J* = 15.5 Hz, 1H), 3.76 (*d*, *J* = 15.3 Hz, 1H), 3.71 (*s*, 2H), 3.55–3.49 (*m*, 1H), 3.20 (*q*, *J* = 7.2 Hz, 1H), 2.35 (*s*, 3H), 1.36 (*d*, *J* = 7.2 Hz, 3H), 1.08 (*d*, *J* = 6.4 Hz, 3H); ^{13}C{^{1}H} NMR (176 MHz, $CDCl_3$) δ 208.8, 156.5 (*q*, *J* = 36.5 Hz), 154.7, 152.3, 149.9, 148.6, 116.3 (q, *J* = 289.0 Hz), 111.4, 109.9, 109.8, 109.6, 57.2, 56.9, 53.3, 49.6, 44.7, 42.8, 42.0, 15.7, 12.9; HRMS (ESI) *m*/*z*: $[M + H]^+$ 411.; Analysis calculated for $C_{20}H_{21}F_3N_2O_4$ %: C 58.53, H 5.16, N 6.83. Found: C 58.54, H 5.17, N 6.83.

6. Refinement

Crystal data, data collection and structure refinement details are summarized in Table 3. Carbon-bound H atoms were placed in calculated positions [C—H = 0.95–1.00 Å; U_{iso}(H) = 1.2 or 1.5U_{eq}(C)] and were included in the refinement in the riding-model approximation. Owing to poor agreement between observed and calculated intensities, twenty three outliers (0 0 6, 4 0 12, 5 1 6, 3 6 3, 4 8 5, 4 5 5, 12 11 0, 0 6 3, 4 7 5, 1 0 8, 1 1 2, 0 4 9, 6 5 2, 4 8 0, 3 6 7, 7 1 1, 4 1 9, 5 0 6, 0 0 2, 2 1 7, 4 2 8, 4 4 5, 2 5 5) were omitted during the final refinement cycle.

Acknowledgements

The authors' contributions are as follows. Conceptualization, MA, AAE and AB; synthesis, AAE, MSG and BGMR; X-ray analysis, SÖY and MA; writing (review and editing of the manuscript) SÖY, MA and AB; funding acquisition, AAE and MSG; supervision, MA, AAE and AB.

References

Bernstein, J., Davis, R. E., Shimoni, L. & Chang, N.-L. (1995). *Angew. Chem. Int. Ed. Engl.* **34**, 1555–1573.
Borisova, K. K., Nikitina, E. V., Novikov, R. A., Khrustalev, V. N., Dorovatovskii, P. V., Zubavichus, Y. V., Kuznetsov, M. L., Zaytsev, V. P., Varlamov, A. V. & Zubkov, F. I. (2018). *Chem. Commun.* **54**, 2850–2853.
Cremer, D. & Pople, J. A. (1975). *J. Am. Chem. Soc.* **97**, 1354–1358.
Ema, T., Okuda, K., Watanabe, S., Yamasaki, T., Minami, T., Esipenko, N. A. & Anzenbacher, P. (2014). *Org. Lett.* **16**, 1302–1305.
Farrugia, L. J. (2012). *J. Appl. Cryst.* **45**, 849–854.
Groom, C. R., Bruno, I. J., Lightfoot, M. P. & Ward, S. C. (2016). *Acta Cryst*. B**72**, 171–179.
Guchhait, T. & Mani, G. (2011). *J. Org. Chem.* **76**, 10114–10121.
Gurbanov, A. V., Kuznetsov, M. L., Demukhamedova, S. D., Alieva, I. N., Godjaev, N. M., Zubkov, F. I., Mahmudov, K. T. & Pombeiro, A. J. L. (2020*a*). *CrystEngComm*, **22**, 628–633.
Gurbanov, A. V., Kuznetsov, M. L., Mahmudov, K. T., Pombeiro, A. J. L. & Resnati, G. (2020*b*). *Chem. Eur. J.* **26**, 14833–14837.
Hathwar, V. R., Sist, M., Jørgensen, M. R. V., Mamakhel, A. H., Wang, X., Hoffmann, C. M., Sugimoto, K., Overgaard, J. & Iversen, B. B. (2015). *IUCrJ*, **2**, 563–574.
Ivanova, L., Skjerve, E., Eriksen, G. S. & Uhlig, S. (2006). *Toxicon*, **47**, 868–876.
Jana, D., Guchhait, T., Subramaniyan, V., Kumar, A. & Mani, G. (2019). *Tetrahedron Lett.* **60**, 151247–151250.
Khabibullina, G. R., Fedotova, E. S., Tyumkina, T. V., Abdullin, M. F., Ibragimov, A. G. & Dzhemilev, U. M. (2018). *Chem. Heterocycl. C.* **54**, 744–750.
Khalilov, A. N., Tüzün, B., Taslimi, P., Tas, A., Tuncbilek, Z. & Cakmak, N. K. (2021). *J. Mol. Liq.* **344**, 117761.
Krishna, G., Grudinin, D. G., Nikitina, E. V. & Zubkov, F. I. (2022). *Synthesis*, **54**, 797–863.
Kvyatkovskaya, E. A., Borisova, K. K., Epifanova, P. P., Senin, A. A., Khrustalev, V. N., Grigoriev, M. S., Bunev, A. S., Gasanov, R. E.,

Polyanskii, K. B. & Zubkov, F. I. (2021*a*). *New J. Chem.* **45**, 19497–19505.
Kvyatkovskaya, E. A., Epifanova, P. P., Nikitina, E. V., Senin, A. A., Khrustalev, V. N., Polyanskii, K. B. & Zubkov, F. I. (2021*b*). *New J. Chem.* **45**, 3400–3407.
Levy, D., Bluzat, A., Seigneuret, M. & Rigaud, J.-L. (1995). *Biochem. Pharmacol.* **50**, 2105–2107.
Ma, Z., Mahmudov, K. T., Aliyeva, V. A., Gurbanov, A. V., Guedes da Silva, M. F. C. & Pombeiro, A. J. L. (2021). *Coord. Chem. Rev.* **437**, 213859.
Maharramov, A. M., Aliyeva, R. A., Aliyev, I. A., Pashaev, F. G., Gasanov, A. G., Azimova, S. I., Askerov, R. K., Kurbanov, A. V. & Mahmudov, K. T. (2010). *Dyes Pigments*, **85**, 1–6.
Mahmoudi, G., Bauzá, A., Gurbanov, A. V., Zubkov, F. I., Maniukiewicz, W., Rodríguez-Diéguez, A., López-Torres, E. & Frontera, A. (2016). *CrystEngComm*, **18**, 9056–9066.
Mahmudov, K. T., Gurbanov, A. V., Aliyeva, V. A., Guedes da Silva, M. F. C., Resnati, G. & Pombeiro, A. J. L. (2022). *Coord. Chem. Rev.* **464**, 214556.
Mahmudov, K. T., Huseynov, F. E., Aliyeva, V. A., Guedes da Silva, M. F. C. & Pombeiro, A. J. L. (2021). *Chem. Eur. J.* **27**, 14370–14389.
Naghiyev, F. N., Cisterna, J., Khalilov, A. N., Maharramov, A. M., Askerov, R. K., Asadov, K. A., Mamedov, I. G., Salmanli, K. S., Cárdenas, A. & Brito, I. (2020). *Molecules*, **25**, 2235–2248.
Rigaku OD (2021). *CrysAlis PRO*. Rigaku Oxford Diffraction, Yarnton, England.
Rivera, A., Nerio, L. S. & Quevedo, R. (2015). *Tetrahedron Lett.* **56**, 6059–6062.
Safavora, A. S., Brito, I., Cisterna, J., Cárdenas, A., Huseynov, E. Z., Khalilov, A. N., Naghiyev, F. N., Askerov, R. K. & Maharramov, A. M. Z. (2019). *Kristallogr. New Cryst. Struct.* **234**, 1183–1185.
Sheldrick, G. M. (2015*a*). *Acta Cryst.* A**71**, 3–8.
Sheldrick, G. M. (2015*b*). *Acta Cryst.* C**71**, 3–8.
Shikhaliyev, N. Q., Ahmadova, N. E., Gurbanov, A. V., Maharramov, A. M., Mammadova, G. Z., Nenajdenko, V. G., Zubkov, F. I., Mahmudov, K. T. & Pombeiro, A. J. L. (2018). *Dyes Pigments*, **150**, 377–381.
Shikhaliyev, N. Q., Kuznetsov, M. L., Maharramov, A. M., Gurbanov, A. V., Ahmadova, N. E., Nenajdenko, V. G., Mahmudov, K. T. & Pombeiro, A. J. L. (2019). *CrystEngComm*, **21**, 5032–5038.
Simonov, Y. A., Dvorkin, A. A., Fonari, M. S., Malinowski, T. I., Luboch, E., Cygan, A., Biernat, J. F., Ganin, E. V. & Popkov, Y. A. (1993). *J. Inclusion Phenom. Mol. Recognit. Chem.* **15**, 79–89.
Spek, A. L. (2020). *Acta Cryst.* E**76**, 1–11.
Turner, M. J., McKinnon, J. J., Wolff, S. K., Grimwood, D. J., Spackman, P. R., Jayatilaka, D. & Spackman, M. A. (2017). *CrystalExplorer17.5*. University of Western Australia.http://hirshfeldsuface.net
Yadigarov, R. R., Khalilov, A. N., Mamedov, I. G., Nagiev, F. N., Magerramov, A. M. & Allakhverdiev, M. A. (2009). *Russ. J. Org. Chem.* **45**, 1856–1858.

supporting information

Acta Cryst. (2023). E**79**, 292-296 [https://doi.org/10.1107/S2056989023001986]

Crystal structure and Hirshfeld surface analysis of (2²*RS*,2³*SR*,2⁵*RS*,2⁶*SR*)-2³,2⁵,5-trimethyl-2¹-(2,2,2-trifluoroacetyl)-5-aza-2(2,6)-piperidina-1,3(2,5)-difuranacyclohexaphan-2⁴-one

Sema Öztürk Yıldırım, Mehmet Akkurt, Anastasia A. Ershova, Mikhail S. Grigoriev, Bruno G.M. Rocha and Ajaya Bhattarai

Computing details

Data collection: *CrysAlis PRO* 1.171.41.117a (Rigaku OD, 2021); cell refinement: *CrysAlis PRO* 1.171.41.117a (Rigaku OD, 2021); data reduction: *CrysAlis PRO* 1.171.41.117a (Rigaku OD, 2021); program(s) used to solve structure: *SHELXT* (Sheldrick, 2015a); program(s) used to refine structure: *SHELXL2018* (Sheldrick, 2015b); molecular graphics: *ORTEP-3 for Windows* (Farrugia, 2012); software used to prepare material for publication: *PLATON* (Spek, 2020).

/ (2²*RS*,2³*SR*,2⁵*RS*,2⁶*SR*)-\ 2³,2⁵,5-trimethyl-2¹-(2,2,2-\ trifluoroacetyl)-5-aza-2(2,6)-piperidina-1,3(2,5)-difuranacyclohexaphan-\ 2⁴-one

Crystal data

$C_{20}H_{21}F_3N_2O_4$
M_r = 410.39
Orthorhombic, *Pbca*
a = 11.1351 (1) Å
b = 17.0545 (2) Å
c = 19.9131 (3) Å
V = 3781.57 (8) Å³
Z = 8
F(000) = 1712
D_x = 1.442 Mg m^{-3}
Cu *Kα* radiation, *λ* = 1.54184 Å
Cell parameters from 15774 reflections
θ = 2.2–78.7°
μ = 1.03 mm^{-1}
T = 100 K
Prism, colourless
0.25 × 0.20 × 0.20 mm

Data collection

XtaLAB Synergy, Dualflex, HyPix diffractometer
Radiation source: micro-focus sealed X-ray tube
φ and *ω* scans
Absorption correction: multi-scan (CrysAlisPro; Rigaku OD, 2021)
T_{min} = 0.761, T_{max} = 0.801
24690 measured reflections
4040 independent reflections
3752 reflections with $I > 2\sigma(I)$
R_{int} = 0.031
θ_{max} = 79.3°, θ_{min} = 5.2°
h = −12→14
k = −20→21
l = −25→25

Refinement

Refinement on F^2
Least-squares matrix: full
$R[F^2 > 2\sigma(F^2)]$ = 0.037
$wR(F^2)$ = 0.102
S = 1.03
4040 reflections
265 parameters
0 restraints
Primary atom site location: difference Fourier map

Secondary atom site location: difference Fourier map	$w = 1/[\sigma^2(F_o^2) + (0.0586P)^2 + 1.2514P]$ where $P = (F_o^2 + 2F_c^2)/3$
Hydrogen site location: inferred from neighbouring sites	$(\Delta/\sigma)_{max} = 0.001$
H-atom parameters constrained	$\Delta\rho_{max} = 0.32$ e Å^{-3}
	$\Delta\rho_{min} = -0.21$ e Å^{-3}

Special details

Experimental. CrysAlisPro 1.171.41.117a (Rigaku OD, 2021) Empirical absorption correction using spherical harmonics, implemented in SCALE3 ABSPACK scaling algorithm.

Geometry. All esds (except the esd in the dihedral angle between two l.s. planes) are estimated using the full covariance matrix. The cell esds are taken into account individually in the estimation of esds in distances, angles and torsion angles; correlations between esds in cell parameters are only used when they are defined by crystal symmetry. An approximate (isotropic) treatment of cell esds is used for estimating esds involving l.s. planes.

Fractional atomic coordinates and isotropic or equivalent isotropic displacement parameters (Å^2)

	x	*y*	*z*	U_{iso}*/U_{eq}
F1	0.46254 (7)	0.40849 (4)	0.69241 (4)	0.03490 (19)
F2	0.47797 (8)	0.35558 (4)	0.59393 (4)	0.0394 (2)
F3	0.62779 (7)	0.41697 (5)	0.63772 (5)	0.0411 (2)
C1	0.25270 (10)	0.46229 (6)	0.61741 (6)	0.0228 (2)
H1	0.2891	0.4136	0.6366	0.027*
C2	0.18508 (10)	0.50270 (6)	0.67299 (6)	0.0234 (2)
C3	0.06815 (11)	0.52036 (7)	0.68327 (6)	0.0269 (2)
H3	0.0021	0.5056	0.6559	0.032*
C4	0.06377 (11)	0.56583 (7)	0.74372 (6)	0.0287 (3)
H4	−0.0059	0.5875	0.7641	0.034*
C5	0.17741 (11)	0.57194 (7)	0.76607 (6)	0.0264 (2)
C6	0.23342 (11)	0.61600 (7)	0.82269 (6)	0.0291 (3)
H6A	0.1701	0.6439	0.8481	0.035*
H6B	0.2730	0.5786	0.8536	0.035*
N7	0.32220 (10)	0.67275 (6)	0.79832 (5)	0.0295 (2)
C8	0.27337 (13)	0.73574 (7)	0.75550 (7)	0.0337 (3)
H8A	0.2940	0.7876	0.7747	0.040*
H8B	0.1848	0.7315	0.7532	0.040*
C9	0.32582 (12)	0.72806 (7)	0.68700 (6)	0.0299 (3)
C10	0.42408 (12)	0.75661 (7)	0.65530 (7)	0.0318 (3)
H10	0.4722	0.7997	0.6692	0.038*
C11	0.44143 (11)	0.70908 (7)	0.59651 (6)	0.0286 (3)
H11	0.5035	0.7143	0.5641	0.034*
C12	0.35196 (10)	0.65556 (7)	0.59651 (6)	0.0246 (2)
C13	0.32223 (10)	0.58544 (6)	0.55457 (6)	0.0230 (2)
H13	0.3733	0.5873	0.5133	0.028*
C14	0.18934 (10)	0.58564 (6)	0.53217 (6)	0.0247 (2)
H14	0.1393	0.5980	0.5725	0.030*
C15	0.15409 (10)	0.50470 (7)	0.50819 (6)	0.0243 (2)
O15	0.11156 (8)	0.49283 (5)	0.45311 (4)	0.0309 (2)
C16	0.17334 (10)	0.43780 (7)	0.55769 (6)	0.0250 (2)
H16	0.0930	0.4225	0.5759	0.030*

N17	0.35219 (9)	0.51181 (5)	0.59182 (5)	0.0220 (2)
C17	0.47033 (10)	0.49467 (7)	0.59476 (6)	0.0244 (2)
O17	0.54942 (7)	0.53360 (5)	0.56885 (4)	0.0294 (2)
O18	0.25418 (7)	0.53151 (5)	0.72431 (4)	0.02384 (18)
C18	0.50906 (11)	0.41827 (7)	0.63123 (7)	0.0303 (3)
O19	0.27850 (8)	0.66728 (5)	0.65050 (4)	0.02727 (19)
C19	0.39990 (13)	0.70224 (8)	0.85115 (7)	0.0353 (3)
H19A	0.4331	0.6581	0.8766	0.053*
H19B	0.3534	0.7360	0.8813	0.053*
H19C	0.4656	0.7325	0.8312	0.053*
C20	0.16602 (12)	0.64922 (7)	0.48000 (7)	0.0320 (3)
H20A	0.0798	0.6519	0.4704	0.048*
H20B	0.2098	0.6368	0.4387	0.048*
H20C	0.1934	0.6999	0.4974	0.048*
C21	0.22552 (12)	0.36654 (7)	0.52092 (6)	0.0311 (3)
H21A	0.1701	0.3501	0.4854	0.047*
H21B	0.2367	0.3234	0.5528	0.047*
H21C	0.3031	0.3806	0.5011	0.047*

Atomic displacement parameters (Å²)

	U^{11}	U^{22}	U^{33}	U^{12}	U^{13}	U^{23}
F1	0.0367 (4)	0.0339 (4)	0.0340 (4)	0.0041 (3)	−0.0030 (3)	0.0081 (3)
F2	0.0474 (5)	0.0240 (4)	0.0468 (5)	0.0084 (3)	−0.0041 (4)	−0.0032 (3)
F3	0.0281 (4)	0.0407 (4)	0.0544 (5)	0.0110 (3)	−0.0028 (3)	0.0045 (4)
C1	0.0233 (5)	0.0194 (5)	0.0258 (5)	−0.0018 (4)	0.0010 (4)	0.0013 (4)
C2	0.0253 (5)	0.0218 (5)	0.0231 (5)	−0.0035 (4)	−0.0007 (4)	0.0007 (4)
C3	0.0231 (5)	0.0307 (6)	0.0270 (6)	−0.0025 (4)	−0.0004 (4)	0.0010 (5)
C4	0.0246 (6)	0.0337 (6)	0.0279 (6)	0.0002 (5)	0.0034 (4)	−0.0007 (5)
C5	0.0270 (6)	0.0270 (6)	0.0253 (6)	−0.0001 (4)	0.0031 (4)	−0.0018 (4)
C6	0.0297 (6)	0.0311 (6)	0.0266 (6)	−0.0015 (5)	0.0011 (5)	−0.0028 (5)
N7	0.0329 (5)	0.0269 (5)	0.0288 (5)	−0.0024 (4)	−0.0017 (4)	−0.0021 (4)
C8	0.0418 (7)	0.0249 (6)	0.0345 (7)	0.0014 (5)	−0.0018 (5)	−0.0041 (5)
C9	0.0377 (7)	0.0207 (5)	0.0313 (6)	−0.0007 (5)	−0.0051 (5)	−0.0011 (4)
C10	0.0389 (7)	0.0211 (5)	0.0353 (7)	−0.0056 (5)	−0.0071 (5)	0.0025 (5)
C11	0.0300 (6)	0.0228 (5)	0.0330 (6)	−0.0038 (4)	−0.0018 (5)	0.0053 (5)
C12	0.0266 (5)	0.0205 (5)	0.0268 (5)	0.0005 (4)	−0.0016 (4)	0.0033 (4)
C13	0.0233 (5)	0.0200 (5)	0.0256 (5)	−0.0008 (4)	0.0005 (4)	0.0030 (4)
C14	0.0245 (5)	0.0228 (5)	0.0268 (6)	0.0003 (4)	−0.0011 (4)	0.0016 (4)
C15	0.0198 (5)	0.0262 (5)	0.0269 (6)	−0.0006 (4)	0.0016 (4)	−0.0010 (4)
O15	0.0305 (4)	0.0344 (5)	0.0278 (4)	−0.0005 (4)	−0.0040 (4)	−0.0028 (3)
C16	0.0263 (5)	0.0222 (5)	0.0265 (6)	−0.0048 (4)	0.0011 (4)	−0.0007 (4)
N17	0.0222 (5)	0.0185 (4)	0.0255 (5)	0.0001 (3)	0.0014 (4)	0.0017 (3)
C17	0.0236 (5)	0.0239 (5)	0.0258 (6)	0.0011 (4)	0.0004 (4)	−0.0019 (4)
O17	0.0234 (4)	0.0325 (4)	0.0322 (5)	−0.0013 (3)	0.0020 (3)	0.0012 (3)
O18	0.0223 (4)	0.0246 (4)	0.0246 (4)	−0.0010 (3)	0.0001 (3)	−0.0021 (3)
C18	0.0290 (6)	0.0270 (6)	0.0349 (6)	0.0049 (5)	−0.0005 (5)	0.0008 (5)
O19	0.0299 (4)	0.0235 (4)	0.0284 (4)	−0.0026 (3)	0.0005 (3)	−0.0017 (3)

C19	0.0393 (7)	0.0340 (6)	0.0326 (7)	−0.0059 (5)	−0.0025 (5)	−0.0057 (5)
C20	0.0332 (6)	0.0273 (6)	0.0355 (6)	0.0005 (5)	−0.0059 (5)	0.0059 (5)
C21	0.0407 (7)	0.0219 (5)	0.0307 (6)	−0.0039 (5)	0.0015 (5)	−0.0030 (5)

Geometric parameters (Å, º)

F1—C18	1.3344 (15)	C11—C12	1.3511 (16)
F2—C18	1.3470 (15)	C11—H11	0.9500
F3—C18	1.3286 (15)	C12—O19	1.3655 (14)
C1—N17	1.4833 (14)	C12—C13	1.4958 (15)
C1—C2	1.5056 (16)	C13—N17	1.4961 (13)
C1—C16	1.5393 (16)	C13—C14	1.5455 (16)
C1—H1	1.0000	C13—H13	1.0000
C2—C3	1.3521 (17)	C14—C15	1.5125 (16)
C2—O18	1.3702 (14)	C14—C20	1.5239 (16)
C3—C4	1.4328 (17)	C14—H14	1.0000
C3—H3	0.9500	C15—O15	1.2117 (15)
C4—C5	1.3454 (17)	C15—C16	1.5230 (16)
C4—H4	0.9500	C16—C21	1.5333 (16)
C5—O18	1.3776 (14)	C16—H16	1.0000
C5—C6	1.4916 (16)	N17—C17	1.3489 (15)
C6—N7	1.4661 (16)	C17—O17	1.2176 (15)
C6—H6A	0.9900	C17—C18	1.5527 (16)
C6—H6B	0.9900	C19—H19A	0.9800
N7—C19	1.4520 (16)	C19—H19B	0.9800
N7—C8	1.4755 (17)	C19—H19C	0.9800
C8—C9	1.4895 (19)	C20—H20A	0.9800
C8—H8A	0.9900	C20—H20B	0.9800
C8—H8B	0.9900	C20—H20C	0.9800
C9—C10	1.3537 (19)	C21—H21A	0.9800
C9—O19	1.3713 (14)	C21—H21B	0.9800
C10—C11	1.4370 (18)	C21—H21C	0.9800
C10—H10	0.9500		

N17—C1—C2	111.43 (9)	N17—C13—H13	107.9
N17—C1—C16	108.54 (9)	C14—C13—H13	107.9
C2—C1—C16	113.89 (9)	C15—C14—C20	112.95 (10)
N17—C1—H1	107.6	C15—C14—C13	109.73 (9)
C2—C1—H1	107.6	C20—C14—C13	111.19 (10)
C16—C1—H1	107.6	C15—C14—H14	107.6
C3—C2—O18	110.37 (10)	C20—C14—H14	107.6
C3—C2—C1	134.01 (11)	C13—C14—H14	107.6
O18—C2—C1	115.57 (10)	O15—C15—C14	122.66 (11)
C2—C3—C4	106.29 (10)	O15—C15—C16	121.05 (10)
C2—C3—H3	126.9	C14—C15—C16	116.28 (10)
C4—C3—H3	126.9	C15—C16—C21	109.76 (10)
C5—C4—C3	106.73 (11)	C15—C16—C1	112.18 (9)
C5—C4—H4	126.6	C21—C16—C1	111.50 (10)

C3—C4—H4	126.6	C15—C16—H16	107.7
C4—C5—O18	110.19 (10)	C21—C16—H16	107.7
C4—C5—C6	133.02 (11)	C1—C16—H16	107.7
O18—C5—C6	116.68 (10)	C17—N17—C1	126.16 (9)
N7—C6—C5	111.36 (10)	C17—N17—C13	114.89 (9)
N7—C6—H6A	109.4	C1—N17—C13	118.79 (9)
C5—C6—H6A	109.4	O17—C17—N17	124.67 (11)
N7—C6—H6B	109.4	O17—C17—C18	117.06 (11)
C5—C6—H6B	109.4	N17—C17—C18	118.23 (10)
H6A—C6—H6B	108.0	C2—O18—C5	106.33 (9)
C19—N7—C6	113.00 (10)	F3—C18—F1	107.18 (11)
C19—N7—C8	112.71 (10)	F3—C18—F2	107.23 (10)
C6—N7—C8	115.05 (10)	F1—C18—F2	107.72 (10)
N7—C8—C9	108.70 (10)	F3—C18—C17	109.62 (10)
N7—C8—H8A	109.9	F1—C18—C17	115.10 (10)
C9—C8—H8A	109.9	F2—C18—C17	109.68 (10)
N7—C8—H8B	109.9	C12—O19—C9	107.32 (9)
C9—C8—H8B	109.9	N7—C19—H19A	109.5
H8A—C8—H8B	108.3	N7—C19—H19B	109.5
C10—C9—O19	109.59 (11)	H19A—C19—H19B	109.5
C10—C9—C8	135.42 (12)	N7—C19—H19C	109.5
O19—C9—C8	113.66 (11)	H19A—C19—H19C	109.5
C9—C10—C11	106.59 (11)	H19B—C19—H19C	109.5
C9—C10—H10	126.7	C14—C20—H20A	109.5
C11—C10—H10	126.7	C14—C20—H20B	109.5
C12—C11—C10	106.38 (11)	H20A—C20—H20B	109.5
C12—C11—H11	126.8	C14—C20—H20C	109.5
C10—C11—H11	126.8	H20A—C20—H20C	109.5
C11—C12—O19	110.05 (10)	H20B—C20—H20C	109.5
C11—C12—C13	134.69 (11)	C16—C21—H21A	109.5
O19—C12—C13	115.09 (10)	C16—C21—H21B	109.5
C12—C13—N17	110.17 (9)	H21A—C21—H21B	109.5
C12—C13—C14	111.80 (9)	C16—C21—H21C	109.5
N17—C13—C14	111.01 (9)	H21A—C21—H21C	109.5
C12—C13—H13	107.9	H21B—C21—H21C	109.5

N17—C1—C2—C3	125.68 (14)	O15—C15—C16—C21	42.86 (15)
C16—C1—C2—C3	2.49 (18)	C14—C15—C16—C21	−137.91 (10)
N17—C1—C2—O18	−51.30 (13)	O15—C15—C16—C1	167.40 (11)
C16—C1—C2—O18	−174.48 (9)	C14—C15—C16—C1	−13.37 (14)
O18—C2—C3—C4	2.27 (13)	N17—C1—C16—C15	−40.88 (12)
C1—C2—C3—C4	−174.82 (12)	C2—C1—C16—C15	83.87 (12)
C2—C3—C4—C5	−0.54 (14)	N17—C1—C16—C21	82.69 (11)
C3—C4—C5—O18	−1.37 (14)	C2—C1—C16—C21	−152.56 (10)
C3—C4—C5—C6	174.71 (13)	C2—C1—N17—C17	116.85 (12)
C4—C5—C6—N7	−118.73 (15)	C16—C1—N17—C17	−116.96 (12)
O18—C5—C6—N7	57.15 (14)	C2—C1—N17—C13	−67.88 (12)
C5—C6—N7—C19	−165.25 (11)	C16—C1—N17—C13	58.31 (12)

C5—C6—N7—C8	63.35 (13)	C12—C13—N17—C17	−75.59 (12)
C19—N7—C8—C9	112.65 (12)	C14—C13—N17—C17	160.03 (10)
C6—N7—C8—C9	−115.81 (12)	C12—C13—N17—C1	108.62 (11)
N7—C8—C9—C10	−90.45 (17)	C14—C13—N17—C1	−15.77 (13)
N7—C8—C9—O19	74.55 (13)	C1—N17—C17—O17	174.16 (11)
O19—C9—C10—C11	−1.95 (14)	C13—N17—C17—O17	−1.27 (17)
C8—C9—C10—C11	163.48 (14)	C1—N17—C17—C18	−3.30 (17)
C9—C10—C11—C12	0.47 (14)	C13—N17—C17—C18	−178.73 (10)
C10—C11—C12—O19	1.19 (13)	C3—C2—O18—C5	−3.10 (12)
C10—C11—C12—C13	−173.65 (12)	C1—C2—O18—C5	174.59 (9)
C11—C12—C13—N17	103.88 (15)	C4—C5—O18—C2	2.73 (13)
O19—C12—C13—N17	−70.77 (12)	C6—C5—O18—C2	−174.06 (10)
C11—C12—C13—C14	−132.19 (14)	O17—C17—C18—F3	11.43 (15)
O19—C12—C13—C14	53.16 (13)	N17—C17—C18—F3	−170.92 (10)
C12—C13—C14—C15	−163.52 (9)	O17—C17—C18—F1	132.31 (12)
N17—C13—C14—C15	−40.06 (12)	N17—C17—C18—F1	−50.03 (15)
C12—C13—C14—C20	70.80 (12)	O17—C17—C18—F2	−106.05 (12)
N17—C13—C14—C20	−165.74 (10)	N17—C17—C18—F2	71.60 (14)
C20—C14—C15—O15	−0.18 (16)	C11—C12—O19—C9	−2.39 (13)
C13—C14—C15—O15	−124.85 (12)	C13—C12—O19—C9	173.57 (9)
C20—C14—C15—C16	−179.39 (10)	C10—C9—O19—C12	2.69 (13)
C13—C14—C15—C16	55.94 (13)	C8—C9—O19—C12	−166.19 (10)

Hydrogen-bond geometry (Å, º)

*Cg*2 is the centroid of the O19/C9–C12 ring.

D—H···*A*	*D*—H	H···*A*	*D*···*A*	*D*—H···*A*
C1—H1···F1	1.00	2.23	2.9210 (14)	125
C1—H1···F2	1.00	2.47	3.1341 (14)	123
C3—H3···O15^{i}	0.95	2.51	3.3809 (15)	152
C14—H14···O19	1.00	2.49	2.9114 (14)	105
C20—H20*B*···F3^{ii}	0.98	2.54	3.4700 (16)	160
C21—H21*B*···*Cg*2^{iii}	0.98	2.88	3.7561 (13)	150

Symmetry codes: (i) −*x*, −*y*+1, −*z*+1; (ii) −*x*+1, −*y*+1, −*z*+1; (iii) −*x*+1/2, *y*−1/2, *z*.